JOURNAL OF MATERIALS SCIENCE 29 (1994) 5739–5744

Behaviour of hydrogen in pure aluminium, Al–4 mass % Cu and Al–1 mass % Mg_2Si alloys studied by tritium electron microautoradiography

H. SAITOH*, Y. IIJIMA, K. HIRANO†
Department of Materials Science, Faculty of Engineering, Tohoku University, Sendai 980-77, Japan

The effect of lattice defects and microstructures on hydrogen distribution in pure aluminium, Al–4 mass % Cu and Al–1 mass % Mg_2Si alloys has been studied by tritium electron microautoradiography. It was found that in pure aluminium and both the alloys, dislocations and grain boundaries act as short-circuiting diffusion paths and also as trapping sites for hydrogen. It was found that the Guinier–Preston (GP) zones in the Al–1 mass % Mg_2Si alloy do not act as trapping sites but as repellants for hydrogen, in contrast to the GP zones in the Al–4 mass % Cu alloy in which they act as trapping sites for hydrogen. In the Al–1 mass % Mg_2Si alloy, the interfaces between the matrix lattice and the metastable β′ precipitate and between the matrix lattice and the equilibrium β precipitate, were proved to be strong trapping sites for hydrogen. In the Al–4 mass % Cu alloy, the equilibrium θ precipitate itself has been found to be able to trap hydrogen.

1. Introduction

Tritium electron microautoradiography (tritium EM autoradiography) is a unique technique which provides visual information with high spatial resolution on the interrelationship between hydrogen distribution and microstructures in materials [1]. In this technique, a photographic emulsion is adhered to a tritium-charged specimen to be exposed to the β-rays emitted from tritium in the specimen; information on the tritium distribution in the specimen can then be obtained as an autoradiograph.

Tritium emits only low-energy β-rays with a continuous energy spectrum (maximum energy 18.6 keV) with a half-life of 12.3 year [2]. The maximum range of the β-rays of tritium through photographic emulsion and aluminium is 2.5 and 2.7 μm, respectively, and 99% of the energy is absorbed on passing through these materials by about 0.4 μm [3]. Thus, the spatial resolution on the autoradiograph is higher than 1 μm, which is higher in comparison with other methods, such as secondary ion mass spectroscopy (SIMS) [4]. Hence, tritium EM autoradiography may be used effectively to examine the trapping sites of hydrogen and to elucidate the mechanism of the hydrogen embrittlement in steels [5–7]. However, there are only a few reports [8–11] on application of the autoradiographic technique to study hydrogen distribution in pure aluminium and aluminium alloys. Foster *et al.* [8] applied optical-microscopic autoradiography to study hydrogen distribution in pure aluminium and observed the hydrogen segregation on the grain boundary. The present authors have applied the tritium EM autoradiography to an aluminium-rich Al–Mg_2Si alloy [9], a eutectic Al–Cu alloy [10] and an Al–Zn–Mg alloy [11], and observed the hydrogen trapping by the precipitates and the eutectic structure in these alloys.

It is known that the hydrogen embrittlement in aluminium alloys is related to the hydrogen trapping by lattice defects and is also affected by ageing conditions [12, 13]. However, interactions between hydrogen and microstructures in aluminium alloys are still poorly understood. In the present work, the interrelationship between hydrogen distribution and microstructures with lattice defects and precipitates in pure aluminium, Al–4 mass % Cu and Al–1 mass % Mg_2Si alloys was studied by tritium EM autoradiography. In both the Al–4 mass % Cu and Al–1 mass % Mg_2Si alloys, a wide variation of metallographic microstructures, such as the Guinier–Preston (GP) zones, metastable and equilibrium precipitates, can be formed by appropriate heat treatments [14, 15]. Therefore, it is also interesting to examine the interrelationship between hydrogen and those microstructures. It is noted that much attention has been devoted to the behaviour of hydrogen in Al–Mg–Si alloy because this alloy is a candidate for the first wall materials in fusion reactors [16].

2. Experimental procedure

Rod ingots, 15 mm diameter, of Al–1 mass % Mg_2Si quasi binary alloy and Al–4 mass % Cu alloy were

* *Present address*: Materials Science and Engineering, Muroran Institute of Technology, Muroran 050, Japan.
† *Present address*: Professor Emeritus, Tohoku University, Japan.

0022–2461

prepared by melting aluminium blocks (99.999% purity), magnesium granules (99.9% purity), silicon flakes (99.9% purity) and copper plates (99.99% purity) in a high-frequency furnace in a high-purity argon atmosphere and by casting the melt into steel moulds. The ingots were swaged to 10 mm diameter and were homogenized at 520 °C for 1 wk and then cold-rolled into plates 0.1 or 0.2 mm thickness. The pure aluminium specimens were prepared by cold-rolling an aluminium block (99.999% purity) into plates 0.2 mm thick.

The plate specimens of pure aluminium, 4 mm × 6 mm in size, were sealed in a Pyrex tube with argon gas and were annealed at 550 °C for 1 h. The plate specimens of Al–Mg_2Si and Al–Cu alloys 4 mm × 6 mm in size were sealed in a Pyrex tube with argon gas and were solution heat treated at 550 °C for 1 h and were quenched into ice–water. The Al–Mg_2Si alloy specimens were aged at 160 °C for 5 h or 300 °C for 21 h to precipitate the needle-shaped GP zones, the rod-like β′ metastable precipitate and the plate-like β equilibrium precipitate, respectively. The Al–Cu alloy specimens were aged at 130 °C for 10^4 min, 200 °C for 10^4 min or 350 °C for 24 h to form the plate-like GP zones, the plate-like θ′ metastable precipitate and the granular θ equilibrium precipitate, respectively. Some of the annealed pure aluminium and as-quenched Al–Mg_2Si alloy specimens, 0.2 mm thick, were cold rolled to 0.1 mm without ageing heat treatment to study the relationship between the dislocation and hydrogen.

Both tritium and hydrogen were charged into the specimen at room temperature by the cathode charging method using 0.5N NaOH aqueous solution containing tritium of 2.8×10^{13} Bq m^{-3} (the atomic ratio of tritium to hydrogen was 2.4×10^{-7}) as the electrolyte, the current density and the charging time being 20 mA cm^{-2} and 1 h, respectively. (Hereafter, the word "hydrogen" will be used for both hydrogen and tritium, because usually it is not necessary to distinguish the distribution of tritium from that of hydrogen.) After hydrogen charging, the specimen was kept at room temperature for 3 d to release excessively charged hydrogen of more than the thermally equilibrium concentration.

Discs of 3 mm diameter were cut from the hydrogen-charged specimen, and polished into thin foils by the twin-jet method using 75% HNO_3 aqueous solution. The polishing electrolyte was cooled by ice–water, and a constant voltage between 4 and 6 V was applied. It is noted that the surface corrosion or contamination of the specimen during the hydrogen charging can be eliminated by means of this electrolytic polishing.

A sensitive film made of a monolayer of fine AgBr grains, 0.06 μm diameter, placed on a collodion thin film, was prepared by means of the wire-loop method using the nuclear photographic emulsion "Konica NR-H2" supplied by Konica Corporation. One or two drops of isoamyl acetate was put on one side of the specimen to ensure the adhesion of the sensitive film to the surface of the specimen. The specimen with its sensitive film was kept in a dark box maintained at − 45 °C for 1–2 wk to expose the sensitive film to the β-rays emitted from tritium in the specimen.

After exposure, the sensitive film stuck to the surface of the specimen was developed, to turn the AgBr grains exposed by the β-rays into the metallic silver grains. (The developed film is called an autoradiograph.) Thus, information on the distribution of hydrogen in the specimen could be obtained by observing the distribution of the silver grains in the autoradiograph.

In order to observe both the hydrogen distribution and the microstructures of the specimen, the specimen and the autoradiograph adhered to it were observed simultaneously by transmission electron microscopy, (TEM, Jeol-200B) at an acceleration voltage of 200 kV.

3. Results and discussion

3.1. Dislocation

In the autoradiograph of both the well-annealed pure aluminium and solution heat-treated Al–Mg_2Si alloy, it was very rare to observe silver grains in the regions where there was no dislocation if there was a grain boundary within the field of vision. This may indicate that the thermal equilibrium concentration of tritium in both the matrix lattice and grain boundaries was insufficient to produce a latent image in the sensitive film under the present experimental conditions, because the matrix and grain boundaries in the specimen have very weak trapping power for hydrogen. Therefore, hydrogen distribution in the cold-rolled specimens was investigated to examine the interrelationship between dislocations and hydrogen. The interrelationship between hydrogen and the grain boundary will be discussed in a later section.

Fig. 1 shows a tritium EM autoradiograph of cold-rolled pure aluminium. Silver grains may be observed on the cell boundary in the specimen, indicating that hydrogen accumulates on the cell boundaries. Fig. 2 shows a tritium EM autoradiograph of the Al–1 mass % Mg_2Si alloy which was cold rolled after

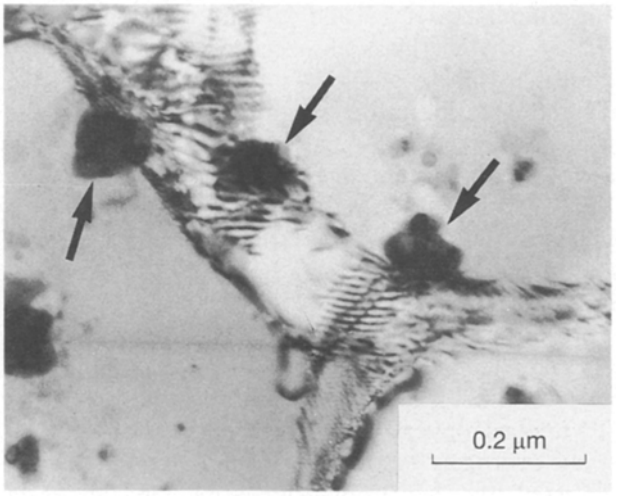

Figure 1 Tritium EM autoradiograph of cold-rolled pure aluminium. Silver grains are observed on the cell boundary, as indicated by arrows.

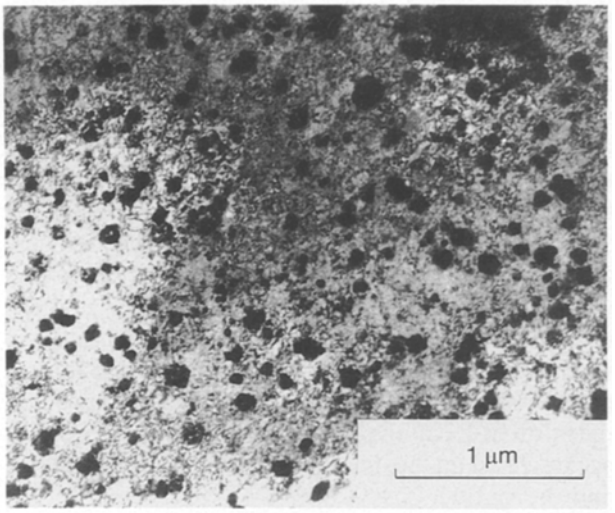

Figure 2 Tritium EM autoradiograph of cold-rolled Al–1 mass % Mg_2Si alloy taken after the solution heat treatment. Many silver grains are observed at the end of the dislocation.

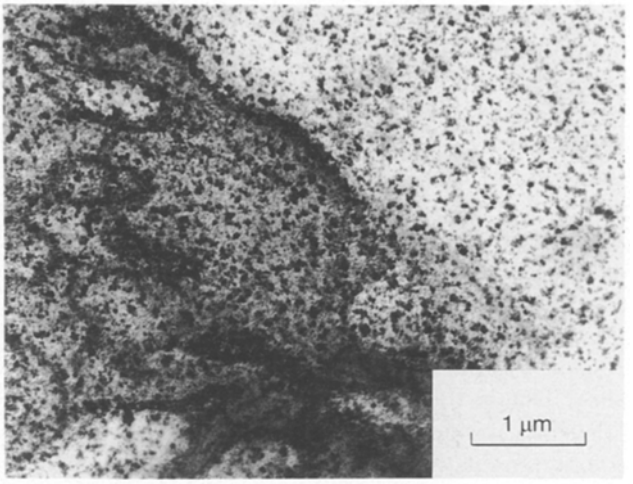

Figure 3 Tritium EM autoradiograph of Al–4 mass % Cu alloy aged at 130 °C for 10^4 min after quenching. Densely distributed silver grains are observed on the GP zones.

the solution heat treatment. Many silver grains are observed at the end of the dislocation. These results suggest that hydrogen accumulates when dislocations are introduced into the specimen, that is, dislocations act as a trapping site for hydrogen in pure aluminium and Al–Mg_2Si alloy. Moreover, the fact that silver grains were observed at the end of the dislocation implies that hydrogen in the interior of the matrix lattice moves to the surface of the specimen along the dislocation by short-circuiting diffusion. Now we consider the migration of hydrogen in a crystal lattice containing a dislocation. When hydrogen in the matrix lattice moves across a dislocation line, the dislocation acts as a trapping site for hydrogen because the potential energy for hydrogen at a dislocation is lower than that in the perfect lattice. On the other hand, when hydrogen moves along a dislocation line, the dislocation acts as a short-circuiting diffusion path, because the potential energy along the dislocation line is lower than that in the matrix. Therefore, the dislocation acts as a trapping site or a short-circuiting diffusion path for hydrogen, depending on its direction of movement. However, in the macroscopic view, a dislocation appears to be only a trapping site for hydrogen, because the network or tangled dislocations cause effectively a long diffusion path.

3.2. GP Zones

Fig. 3 shows a tritium EM autoradiograph of Al–4 mass % Cu alloy aged at 130 °C for 10^4 min after quenching. It has been known that under this ageing condition a large number of fine plate-like GP zones is formed [15]. In Fig. 3, densely distributed silver grains are observed on the GP zones, indicating that the GP zones in the Al–Cu alloy act as a trapping site for hydrogen.

Fig. 4 shows a tritium EM autoradiograph of Al–1 mass % Mg_2Si alloy aged at 160 °C for 5 h after quenching. It is known that a high density of needle-like GP zones and also a small number of the rod-like

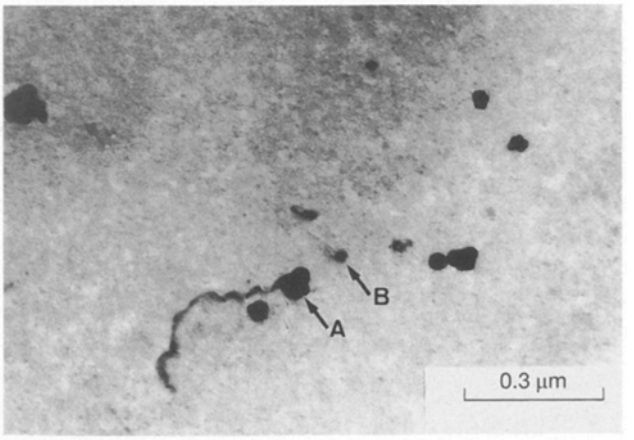

Figure 4 Tritium EM autoradiograph of Al–1 mass % Mg_2Si alloy aged at 160 °C for 5 h after quenching. Silver grains are found to be located at one end of dislocation line (arrow A) and of rod-like β′ phase (arrow B). No definite correlation between distribution of silver grains and that of GP zones was found.

β′ precipitates are formed [14]. In Fig. 4, the silver grains are found at one end of a dislocation line (arrow A) and at one end of a small rod-like precipitate of the β′ phase (arrow B); however, no definite correlation is found between the distribution of the silver grains and that of the GP zones. This result indicates that the GP zones in Al–Mg_2Si alloy have no trapping power for hydrogen in contrast to the GP zones in the Al–Cu alloy.

In metal–hydrogen systems, hydride is formed if the metal has a negative enthalpy of solution for hydrogen [17]. Neither of the element atoms of the GP zones in the Al–Cu alloy forms a hydride at room temperature, because both the elements, aluminium and copper, have positive enthalpies of solution [17]. Therefore, it is concluded that the hydrogen trapping by the GP zones in the Al–Cu alloy is not due to the chemical binding between hydrogen and the elements of the alloy. On the other hand, one of the element atoms, magnesium, of the GP zones in the Al–Mg_2Si alloy can form magnesium hydride, because magnesium has

a negative enthalpy of solution for hydrogen. However, in the case of aged Al–Mg–Si alloy, almost all the magnesium atoms are bonded by the strong ionic bonding [15] with silicon atoms to form the GP zones, and the remaining magnesium atoms, as the solute in the matrix, do not form a hydride, as shown in Fig. 4.

In both the Al–Cu and Al–Mg_2Si alloys, coherency of the GP zones with the matrix lattice causes an elastic stress field in the matrix [15]. The distortion of the matrix around the GP zones was estimated to be − 11.8% in the Al–Cu alloy and 2% in the Al–Mg_2Si alloy. That is, the stress field of the matrix around the GP zones is extensive in the Al–Cu alloy, while it is compressive in the Al–Mg_2Si alloy. It is well known as the Gorsky effect [18] that hydrogen dissolved in metallic crystals moves from a region of compressive elastic stress field to that of tensile elastic stress field. Analogously, it is expected that in the Al–Cu alloy, hydrogen will be attracted to the region affected by the tensile elastic field around the GP zones; on the other hand, in the Al–Mg_2Si alloy, hydrogen will be repelled from the region affected by the compressive elastic field around the GP zones.

Pressouyre [19] suggested the existence of a repellant for hydrogen diffusion in metals. Diffusion of hydrogen in metals should be retarded by a repellant as in the case of a trapping site. However, only a little experimental evidence has been obtained for the existence of the repellant for hydrogen to date [11], thus the present result provides additional experimental evidence.

3.3. The metastable precipitate

On ageing the Al–1 mass % Mg_2Si alloy at 300 °C for 21 h after quenching, both the rod-like β′ metastable precipitate and the plate-like β equilibrium precipitate are formed. Fig. 5 shows a tritium EM autoradiograph of a region around the β′ precipitate in this heat-treated alloy. The silver grains are observed at the end of most of all the rod-like β′ precipitates and are observed along the circular interface between the matrix and the rod-like β′ precipitates. This indicates that hydrogen is trapped along the interface between the rod-like β′ precipitate and the matrix, but not trapped by the β′ precipitate itself.

Because the metastable β′ precipitate is semi-coherent to the matrix, it has interfacial dislocations at the interfaces between it and the matrix lattice. As mentioned in the previous section, the dislocation acts as a trapping site as well as a short-circuiting diffusion path for hydrogen. Thus hydrogen must be trapped by the misfit dislocations around the β′ precipitates and is accumulated on the interfaces between the precipitates and the matrix.

Fig. 6 shows a tritium EM autoradiograph of the Al–4 mass % Cu alloy aged at 200 °C for 10^4 min after quenching in order to precipitate the plate-like θ′ precipitate. The silver grains are observed on the edge of some of the plate-like metastable θ′ precipitates; however, no silver grain is observed on many grains of the θ′ precipitate. It seems that the θ′ precipitate is a weak trapping site for hydrogen. The plate-like θ′ precipitate is partially coherent to the matrix lattice, that is, the edge of the plate is incoherent and the surface of the plate is coherent to the matrix lattice. The coherency strain of the θ′ precipitate is weak compared with that of the GP zones. Thus, the incoherent part of the θ′ precipitate may act as a trapping site for hydrogen.

3.4. The equilibrium precipitates

Fig. 7 shows a tritium EM autoradiograph of a region around the plate-like β precipitate in the Al–1 mass % Mg_2Si alloy aged at 300 °C for 21 h after quenching. The silver grains are observed along the edge of the β precipitate indicating that the interface between the β precipitate and the matrix lattice traps hydrogen. Because the β precipitate is incoherent with the matrix

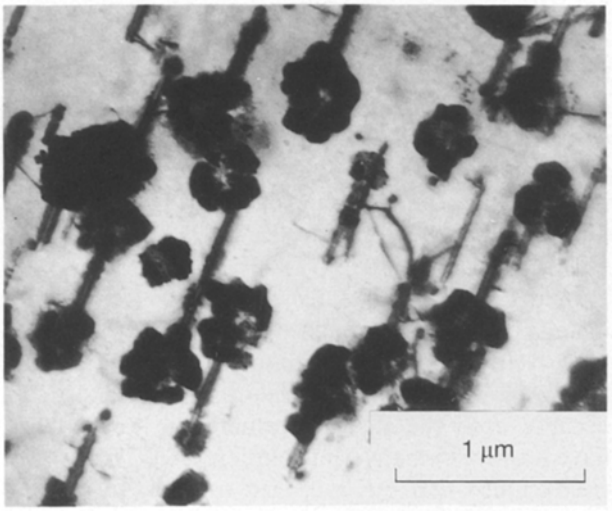

Figure 5 Tritium EM autoradiograph of a region around the β′ precipitate in Al–1 mass % Mg_2Si alloy aged at 300 °C for 21 h after quenching. Silver grains are observed at the end of the rod-like β′ precipitate and are observed along the circular interface between the matrix and the rod-like β′ precipitate.

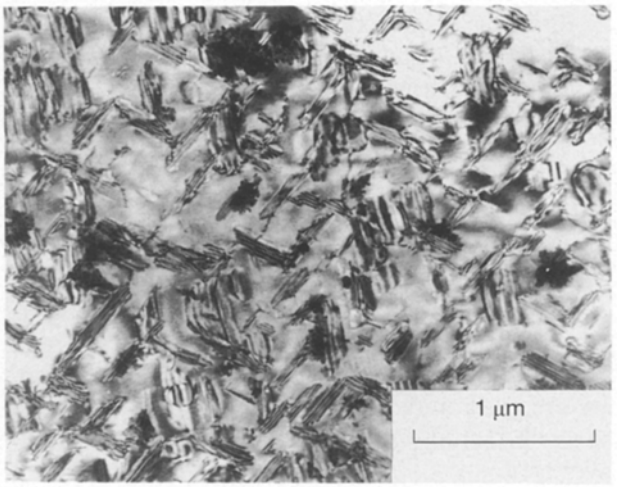

Figure 6 Tritium EM autoradiograph of Al–4 mass % Cu alloy aged at 200 °C for 10^4 min after quenching. Silver grains are observed on the edge of some of the plate-like metastable θ′ precipitates, and are not observed on many grains of θ′ precipitates.

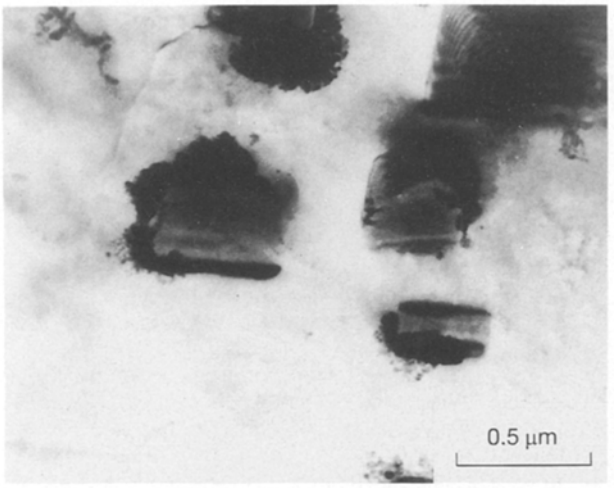

Figure 7 Tritium EM autoradiograph of a region around the β precipitate in Al–1 mass % Mg_2Si alloy aged at 300 °C for 21 h after quenching. Silver grains are observed along the edge of the plate-like equilibrium β precipitate.

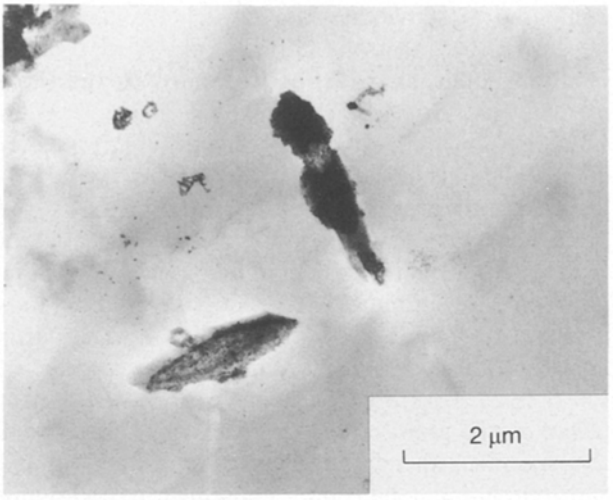

Figure 8 Tritium EM autoradiograph of Al–4 mass % Cu alloy aged at 430 °C for 24 h after quenching. Silver grains are observed on the granular equilibrium θ precipitate.

lattice, many interfacial dislocations exist around it. The interfacial dislocations may trap hydrogen and accumulate it on the interfaces between the β precipitates and the matrix lattice.

Fig. 8 shows a tritium EM autoradiograph of the Al–4 mass % Cu alloy aged at 430 °C for 24 h after quenching to form the granular equilibrium θ precipitate. The silver grains are not always observed along the interface between the matrix lattice and the θ precipitate, and almost all the silver grains are observed on the θ precipitate itself, indicating hydrogen is not trapped by the interface but by the θ precipitate itself. Trapping of the hydrogen by the θ phase was discussed in our previous study [10] of the autoradiograph of a eutectic Al–Cu alloy.

3.5. Grain boundaries

Fig. 9a and b show tritium EM autoradiographs around the large-angle grain boundary of the Al–1 mass % Mg_2Si alloy aged at 300 °C for 21 h after quenching. In Fig. 9a, the silver grains are observed at one end of the rod-like β′ precipitate located both in the matrix and on the grain boundary. However, in Fig. 9b, it is recognized that when the β′ precipitate does not exist, no silver grain is observed on the large-angle grain boundary itself. These results indicate that hydrogen is not accumulated on the large-angle grain boundary itself.

Foster *et al.* [8] observed the hydrogen accumulation on the grain boundary in a bulk aluminium by means of optical-microscopic autoradiography, and Fukushima and Birnbaum [20] reported the segregation of hydrogen on the grain boundary in nickel. These results suggest that the grain boundary in metals has a trapping power for hydrogen. However, the present results obtained by tritium EM autoradiography show that hydrogen is not accumulated on the grain boundary in pure aluminium itself. The difference between the present results and those obtained elsewhere can be explained by considering that

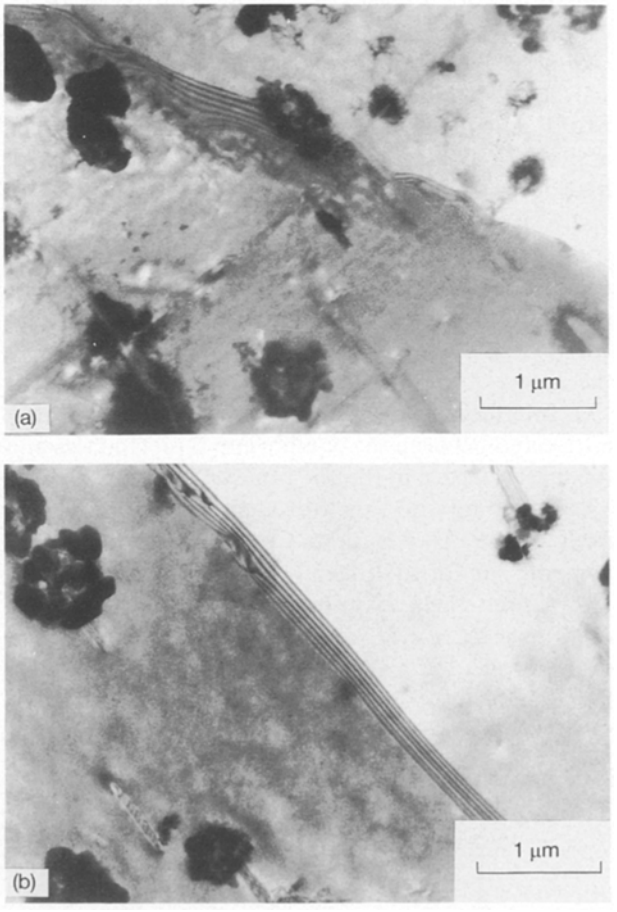

Figure 9 Tritium EM autoradiograph of Al–1 mass % Mg_2Si alloy aged at 300 °C for 21 h after quenching. (a) Silver grains are observed at one end of the β′ precipitate both in the matrix and on the grain boundary. (b) No silver grain is observed on the large-angle grain boundary itself, when the grain boundary precipitate of the β′ does not exist.

the grain boundary acts as the trapping site with low trapping power and, at the same time, as a short-circuiting diffusion path. According to Tsuru and Latanishion [21], the amount of hydrogen moving through the grain boundary in nickel is increased

compared with that moving through the matrix lattice, suggesting that the grain boundary is a short-circuiting diffusion path for hydrogen. In the same way as the hydrogen migration in nickel, a grain boundary in aluminium alloy may act as a short-circuiting diffusion path for hydrogen. When hydrogen in a grain moves to the adjacent grain across the grain boundary, a weak trapping effect appears and hydrogen is attracted to the grain boundary; however, hydrogen moves immediately along the grain boundary, that is, a short-circuiting diffusion occurs. Particularly in the case of a thin-foil specimen, as used in the present work, hydrogen moves from the matrix lattice to the grain boundary and then escapes from the specimen through the grain boundary by the short-circuiting diffusion, consequently avoiding accumulation in the grain boundary.

4. Conclusions

Interactions between hydrogen and the lattice defects and between hydrogen and the precipitates in pure aluminium, Al–4 mass % Cu and Al–1 mass % Mg_2Si alloys have been investigated by the tritium EM autoradiography. The results are summarized as follows.

1. Dislocation in pure aluminium and Al–1 mass % Mg_2Si alloy acts as a trapping site for hydrogen and also acts as a short-circuiting diffusion path for hydrogen.

2. GP zones in the Al–4 mass % Cu alloy act as trapping sites for hydrogen, in contrast to those in Al–1 mass % Mg_2Si alloy, which act as repellants for hydrogen. This difference is attributed to the difference in the stress field around the GP zones in both the alloys.

3. Interfaces between the metastable β′ and matrix lattice and between the equilibrium β precipitates and the matrix lattice in the Al–1 mass % Mg_2Si alloy act as a trapping site for hydrogen. The θ precipitate itself in the Al–4 mass % Cu alloy also acts as a trapping site for hydrogen.

4. A high-angle grain boundary in aluminium and Al–1 mass % Mg_2Si alloy acts simultaneously as a trapping site and a short-circuiting diffusion path for hydrogen.

Acknowledgements

This work was supported by the Grant-in Aid for Fusion Research from the Ministry of Education, Science and Culture. The authors thank Professors K. Kawamura and M. Okamoto, Tokyo Institute of Technology, and Professor M. Nishikawa, Kyushu University, for their continuing interest and encouragement throughout the present work.

References

1. G. R. CASKEY Jr, in "Advanced Techniques for Characterizing Hydrogen in Metals", edited by N. F. Fiore and B. J. Berkowitz (TMS-AIME, Warrendale, PA, 1982) p. 61.
2. C. M. LEDERER and V. S. SHIRLEY (eds), "Tables of Isotopes" (Wiley, New York, 1978) p. 1.
3. J. P. LAURENT and G. LAPASSET, *J. Appl. Rad. Isotopes* **24** (1973) 213.
4. H. K. BIRNBAUM, H. FUKUSHIMA and J. BAKER, in "Advanced Techniques for Characterizing Hydrogen in Metals", edited by N. F. Fiore and B. J. Berkowitz (TMS-AIME, Warrendale, PA, 1982) p. 149.
5. T. ASAOKA, M. LAPASSET, M. AUCOUTURIER and P. LACOMBE, *Corrosion NACE* **34** (1978) 39.
6. H. OHMA, G. P. TIWARI, Y. IIJIMA and K. HIRANO, in "Hydrogen in Metals", Supplement to *Trans. Jpn Inst. Metals* **21** (1980) p. 229.
7. R. CLERMONT, J. OVERJERO-GARCIA, J. CHENE, M. AUCOUTURIER, C. PIRROVANI, P. TISON and J.-P. FIDELLE, *ibid.* p. 233.
8. L. M. FOSTER, T. H. JACK and W. W. HILL, *Met. Trans.* **1** (1970) 3117.
9. H. SAITOH, Y. IIJIMA and K. HIRANO, *J. Jpn Inst. Light Metals* **36** (1986) 286.
10. *Idem, Philos. Mag.* **B64** (1991) 113.
11. Y. IIJIMA, S. YOSHIDA, H. SAITOH, H. TANAKA and K. HIRANO, *J. Mater. Sci.* **27** (1992) 5735.
12. K. HIGASHI, T. OHNISHI, Y. NAKATANI and K. OKABAYASHI, *J. Jpn Inst. Light Metals* **30** (1980) 551.
13. T. OHNISHI, K. HIGASHI, S. SAKURAI and Y. NAKATANI, *ibid.* **33** (1983) 334.
14. G. THOMAS, *J. Inst. Metals* **90** (1961–62) 57.
15. A. KELLY and R. B. NICHOLSON, *Progr. Mater. Sci.* **10** (1961) 148.
16. O. KONNO, S. FUJIKAWA, K. MASUMOTO and M. YAGI, *J. Jpn Inst. Light Metals* **34** (1984) 22.
17. R. SPEISER, in "Metal Hydrides", edited by W. M. Mueller, J. P. Blackledge and G. G. Libowitz (Academic Press, New York, 1968) p. 69.
18. J. VÖLKL, *Ber. Bunsenges. Phys. Chem.* **76** (1972) 797.
19. G. M. PRESSOUYRE, *Met. Trans.* **14A** (1983) 2189.
20. H. FUKUSHIMA and H. K. BIRNBAUM, *Acta Metall.* **32** (1984) 851.
21. T. TSURU and R. M. LATANISHION, *Scripta Metall.* **16** (1982) 575.

Received 10 March 1993
and accepted 22 April 1994.